

## Topological materials for thermoelectric energy conversion

*Yu Pan<sup>#</sup>, Bin He, Federico Serrano-Sanchez, Dong Chen, Chenguang Fu, Walter Schnelle, Gudrun Auffermann, Claudia Felser*

Many good thermoelectric semiconductors have been demonstrated to be topological insulators. The recently discovered class of topological semimetals provides a platform to search for new thermoelectric materials. In our work, we focus on the thermoelectric transport properties of the single crystals of topological semimetals and aim to find materials with advantageous band structure features for high-thermoelectric performance. Because the longitudinal thermoelectric effect, i.e. the Seebeck effect, requires an optimal charge carrier concentration of  $\sim 10^{19} \text{ cm}^{-3}$  near room temperature, we study Dirac/nodal line semimetals with a small density of states.  $\text{YbMnSb}_2$  shows a large Seebeck coefficient over  $160 \mu\text{V K}^{-1}$  and a large power factor of  $2.1 \text{ mW m}^{-1} \text{ K}^{-2}$  at 300 K, which are very high for a semimetal. For highly conductive topological semimetals with large Berry curvature, we investigate their transverse thermoelectric performance, e.g. anomalous Nernst effect (ANE). For example,  $\text{YbMnBi}_2$ ,  $\text{EuMnBi}_2$ , and  $\text{MnBi}$  have been found to show large ANE signals of over a few microvolts per Kelvin. Moreover, beyond the novel topological semimetals, we reveal the band structure of good thermoelectrics including Heusler compounds by angle-resolved photoemission spectroscopy studies of high-quality single crystals. In general, our research interests lie in understanding unusual band structure and thermoelectric transport properties of high-performance single crystals.

Band structure plays an essential role in thermoelectric transport properties. Since the first 3D topological insulators were discovered among  $\text{Bi}_2\text{Te}_3$ -based alloys, the relationship between topological insulators and thermoelectric materials has been a highly attractive area of study. The discoveries of novel topological semimetals have offered a new platform for the investigation of exotic transport properties; for instance, nodal line semimetal  $\text{Mg}_3\text{Bi}_2$ -based compounds have been found to show high thermoelectric performance. [1]

For longitudinal thermoelectric performance, one desirable band structure of a novel semimetal is the combination of highly dispersive Dirac bands with regular bands located slightly below. This band configuration would not only benefit the simultaneous gain of mobility and thermopower, but also make the concentration of the major charge carriers much higher than that of the minor ones. From this point of view, a novel semimetal differs from conventional semimetals in avoiding the equal conduction of two types of charge carriers, making them potentially promising thermoelectric materials.

Those topological semimetals that are highly conductive exhibit low Seebeck coefficients but can be good candidates for a large anomalous Nernst effect (ANE). Topological semimetals with a large Berry curvature are gaining increasing attention in recent years for transverse thermoelectric applications owing to their intrinsic large ANE signals. Beyond the intrinsic contribution, further enhancement in the ANE

performance can be achieved with extrinsic contribution, such as magnon-induced ANE and large spin-orbit coupling (SOC)-related ANE.

Finally, beyond the pursuit of high thermoelectric performance, it is possible to ascertain the band structure features of good thermoelectric materials (including but not limited to topological semimetals) through angle-resolved photoemission spectroscopy (ARPES) technique using high-quality single crystals.

### Longitudinal thermoelectric properties of $\text{YbMnSb}_2$

$\text{YbMnSb}_2$  has been found to be a novel semimetal with a coexistence of a regular hole pocket and 2D Dirac Fermi surfaces near the Fermi level. Most importantly, the 2D Dirac bands show strong anisotropy along different crystal directions while the 3D regular band has less anisotropy. [2] Hence, we investigated  $\text{YbMnSb}_2$ , which has strongly anisotropic 2D Dirac bands and nearly isotropic 3D regular bands, to unveil any unconventional properties. Because of the different anisotropy, 2D Dirac bands and 3D regular bands contribute differently to the electrical transport properties along varied crystal directions. Therefore, by measuring the anisotropic electrical transport properties, the contribution of the Dirac bands to the electrical transport properties can be clearly evidenced.

The thermoelectric transport properties of  $\text{YbMnSb}_2$  along the  $ab$ -plane and  $c$ -axis are shown in Fig. 1. Notably, the  $ab$ -plane direction displays one order of magnitude lower resistivity than the  $c$ -axis, suggesting

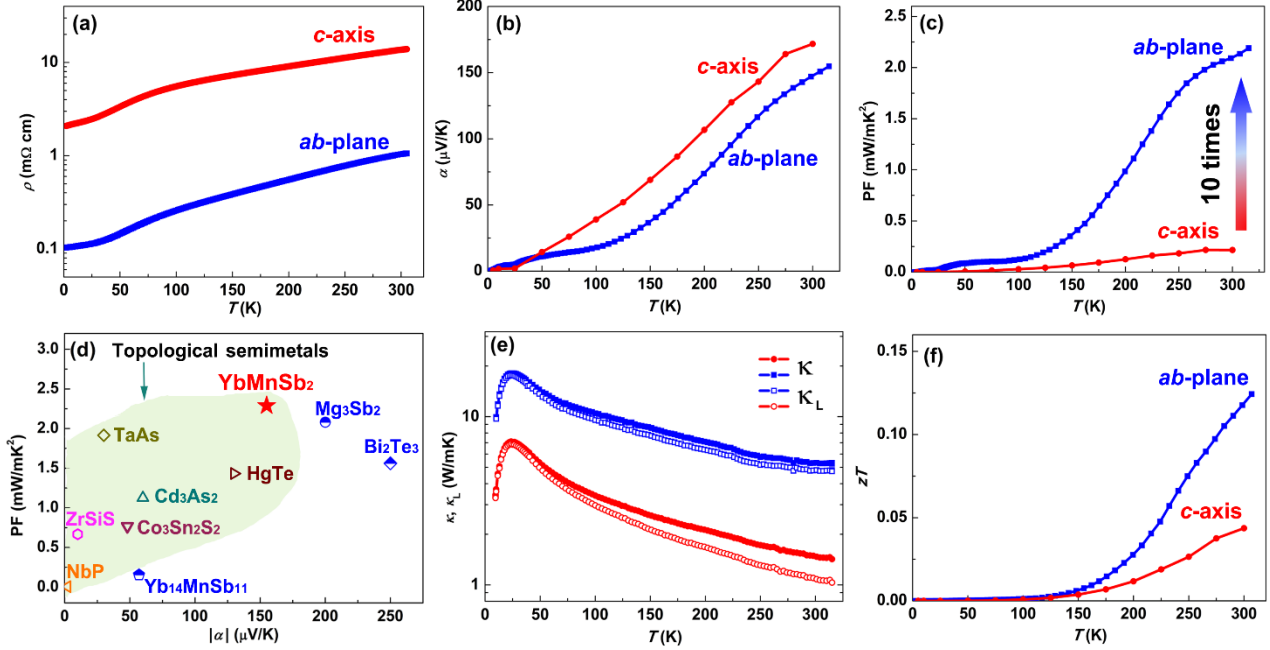


Fig. 1: Temperature dependence of (a) resistivity, (b) Seebeck coefficient, (c) power factor. (d) Comparison of thermopower and power factor of several topological semimetals to high performance thermoelectric semiconductors at 300 K. To avoid the influence of other mechanisms, all the data are taken from single crystals without further doping or alloying. (e) Total and lattice thermal conductivity, and (f)  $zT$  values for  $\text{YbMnSb}_2$  along  $ab$ -plane and  $c$ -axis, respectively.

that the highly dispersive 2D Dirac bands along the  $ab$ -plane significantly enhance the electrical conduction. The thermopower along the  $ab$ -plane and  $c$ -axis exhibits much less anisotropy. At 300 K, a value of  $\approx 160 \mu\text{V K}^{-1}$  is obtained for both the  $ab$ -plane and  $c$ -axis, which is one of the highest values among the presently known novel semimetals and comparable to that of good thermoelectric semiconductors. Consequently, the  $ab$ -plane shows much better electrical performance than the  $c$ -axis, mainly from the highly dispersive Dirac bands guaranteeing a high mobility, and partly also owing to the anisotropic crystal structure. It is worth noting that the power factor along the  $ab$ -plane direction is ten times higher than that of the  $c$ -axis, reaching a value over  $2.1 \text{ mW m}^{-1} \text{ K}^{-2}$  at 300 K (Fig. 1c).

An obvious anisotropy is also observed in thermal conductivity as well as the  $zT$  values, owing to the anisotropic crystal and band structure. Interestingly, the lattice thermal conductivities of  $\text{YbMnSb}_2$  single crystal are quite low, only  $\approx 1 \text{ W m}^{-1} \text{ K}^{-1}$  at 300 K along the  $c$ -axis, which is even lower than that of  $\text{Bi}_2\text{Te}_3$ . No significant bipolar thermal conductivity up to 300 K has been observed in either direction, indicating the negligible contribution of minor charge carriers below 300 K due to the unique band configuration. Consequently, benefitting from the greatly enhanced power factor, a maximum  $zT$  of  $\approx 0.12$  at 300 K is

obtained along the  $ab$ -plane, which is approximately three times higher than that of the  $c$ -axis. This is a good value for a novel semimetal single crystal without any purposeful optimization.

### Large ANE in $\text{YbMnBi}_2$ , $\text{EuMnBi}_2$ , and $\text{MnBi}$

Numerous Mn-based pnictides have been reported to be magnetic topological semimetals. Most importantly, they hold a weakly canted spin structure at the Mn sites, which breaks the time reversal symmetry and gives rise to a non-zero Berry curvature. This non-zero Berry curvature is able to generate an intrinsic ANE signal. Moreover, the heavy pnictogen (particularly Bi)-induced strong SOC can have extra skew forces to the electrons and is beneficial for higher ANE thermopower.

We experimentally investigated two Mn-based magnetic semimetals,  $\text{YbMnBi}_2$  [3] and  $\text{EuMnBi}_2$  [4], and their sister compound, ferromagnetic  $\text{MnBi}$  [5]. We found that a finite canting angle is crucial to generate a large ANE by breaking time reversal symmetry.  $\text{YbMnBi}_2$  is a canted antiferromagnet with a canting temperature of  $T_{sc} = 250 \text{ K}$ . Fig. 2a shows the magnetic field-dependent ANE thermopower of  $\text{YbMnBi}_2$  from 40 K to 260 K. The highest ANE thermopower observed was  $6 \mu\text{V/K}$  at 160 K, which is the highest value among all non-collinear antiferromagnets.

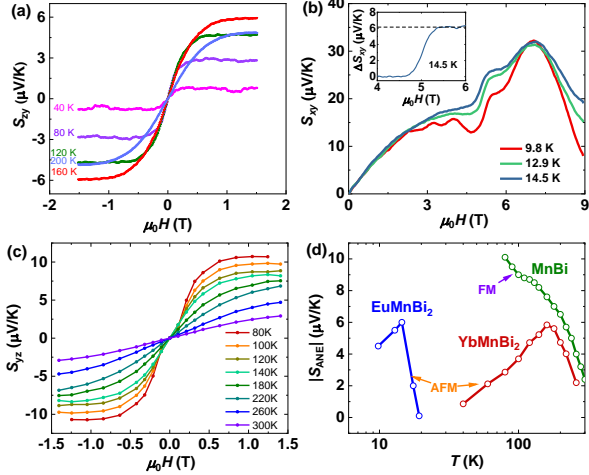


Fig. 2: Magnetic field dependence of the ANE thermopower in (a)  $\text{YbMnBi}_2$ , (b)  $\text{EuMnBi}_2$ , and (c)  $\text{MnBi}$ . The largest ANE signals are 6  $\mu\text{V/K}$  for  $\text{YbMnBi}_2$  and  $\text{EuMnBi}_2$ , and 10  $\mu\text{V/K}$  for  $\text{MnBi}$ . (d) Temperature dependence of the ANE of the three Mn-Bi-based compounds.

Unlike  $\text{YbMnBi}_2$ , which has a natural canting angle at Mn sites below 250 K,  $\text{EuMnBi}_2$  has a more complex magnetic structure because of the inclusion of Eu.  $\text{EuMnBi}_2$  has collinear antiferromagnetic orders of both Mn and Eu at 0 T. However, it has a large canting angle due to a spin-flop transition of Eu below 22 K under a magnetic field of 5 T along the  $c$ -axis because of the coupling of Mn and Eu. This phase transition introduces spin splitting of the massive Dirac cone and breaks time reversal symmetry, resulting in an ANE signal. By subtracting the background, the maximum ANE reaches a value of  $\sim 6 \mu\text{V/K}$  at 14.5 K (inset in Fig. 2b), which vanishes as the temperature becomes close to the transition temperature of 22 K.

In addition, we investigated the ferromagnetic  $\text{MnBi}$ . Though often considered to be a metal,  $\text{MnBi}$  has a much lower carrier density of  $\sim 10^{21}/\text{cm}^3$ , which is close to that of semimetals. In  $\text{MnBi}$ , a giant ANE of 10  $\mu\text{V/K}$  is observed at 80 K, due to both the intrinsic Berry curvature and extrinsic contribution, which we attribute to a strong magnon-electron interaction arising from a strong SOC of Bi. Finally, temperature-dependent ANE thermopowers of the three compounds are shown in Fig. 2d, showing the great potential of Mn-based pnictides for transverse thermoelectric applications.

### Band structure studies of Heusler alloys

Complex band structure, particularly complex Fermi surface with large band degeneracy (number of carrier

pockets)  $N_v$ , benefits the longitudinal thermoelectric performance. ARPES can directly confirm the band degeneracy and reveal the origin of high thermoelectric performance from a band structure viewpoint. Half-Heusler alloys with a valence electron count of 18 have shown promising thermoelectric performance, and are representative systems to study the complex half-Heusler electronic structure. Among them, n-type  $\text{ZrNiSn}$  and p-type  $\text{TiCoSb}$  are remarkable systems in which improved properties have been described by band engineering and phase segregation. Using high-resolution ARPES, the intrinsic band structures of n-type  $\text{ZrNiSn}$  and p-type  $\text{TiCoSb}$  have been revealed.

In the ARPES results of  $\text{ZrNiSn}$  single crystals, a large band-gap of  $0.66 \pm 0.1 \text{ eV}$  has been observed, as shown in Fig. 3a. [6] Additionally, no in-gap states are detected, demonstrating that these are free of enough Ni interstitials defects, which differs from what has been reported in previous studies. Furthermore, a highly anisotropic conduction band has been identified, which results in a large Fermi complexity factor. This is one of the main components from which the high power factor in half-Heusler alloys originates.

For the p-type  $\text{TiCoSb}$ , the energy difference between bands at  $\Gamma$  and L points determined by ARPES is below 0.1 eV (Fig. 3b), which is smaller than that predicted by theoretical calculations. [7] This demonstrates that the band convergence happens at  $\Gamma$  and L points, yielding a high  $N_v$ , which is essential for a high thermoelectric performance. However,  $\text{TiCoSb}$  has also been reported to be a defect-governed transport system. In contrast to  $\text{ZrNiSn}$ , in which no interstitial states are observed,  $\text{TiCoSb}$  displays a diffusive surface in-gap state at L point, demonstrating that  $\text{TiCoSb}$  does have in-gap states originating from Co or Ti interstitials.

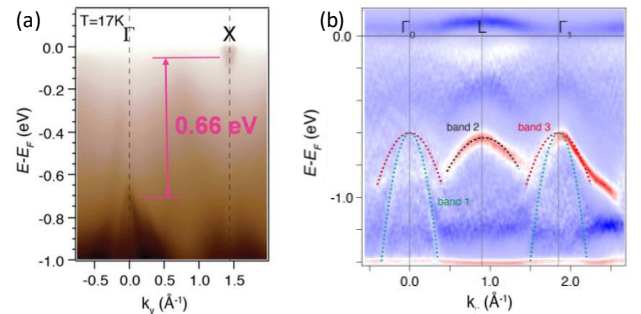


Fig. 3: ARPES intensity plots of (a)  $\text{ZrNiSn}$  electronic structure along  $\Gamma$ -X direction and (b) of  $\text{TiCoSb}$  along  $\Gamma$ -L- $\Gamma$  direction.

## Outlook

Both Zintl compounds and Heusler alloys are large families, which can provide a wide platform to conduct various experiments.  $\text{YbMnSb}_2$ ,  $\text{YbMnBi}_2$ , and  $\text{EuMnBi}_2$  are three members of the  $\text{RMnPn}_2$  Zintl family, where  $R$  is a rare-earth or alkaline-earth metal and  $Pn$  is a pnictide (P, As, Sb, or Bi). There are more  $\text{RMnPn}_2$  compounds, as well as some other 1-1-2 type compounds, which are worthy of investigation of their thermoelectric transport properties.

First, by combining large SOC and ferromagnetism, these compounds are expected to exhibit a large ANE signal. Although only a handful of Bi-based binary magnets exist (e.g.  $\text{MnBi}$ ), the new family of  $\text{RMnBi}_2$  provides abundant compounds. Through finely tuning the Mn-Mn bond distance, it is possible to induce a canted spin structure and thus break the time reversal symmetry. In this case, we can investigate a significant number of magnets with strong SOC, which are decent candidates for giant ANE. Moreover, they are unique systems for revealing the extrinsic contribution from large SOC which have rarely been investigated to date.

Second, other compounds with large ANE are generally ferromagnets with rather low mobility, whereas canted antiferromagnets avoid strong contribution from heavy  $d$  orbitals. For example, benefitting from the large ANE thermopower, sharp dispersion of the  $p_{xy}$  orbitals of Bi, as well as the low thermal conductivity resulting from heavy Bi, the anomalous transverse  $zT$  of  $\text{YbMnBi}_2$  is much higher than that of other compounds with comparable ANE thermopower (Fig. 4). In this case, we assert the importance of the search for more canted antiferromagnets like  $\text{RMnPn}_2$  pnictides for transverse thermoelectric applications.

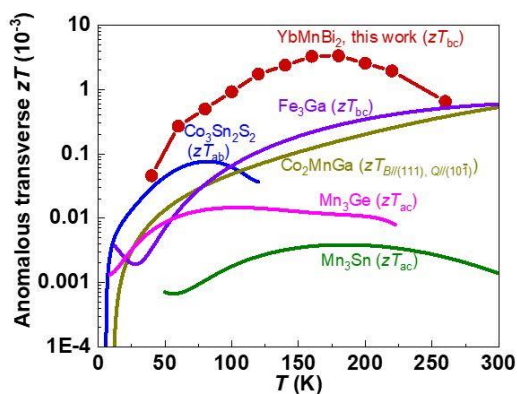


Fig. 4: Anomalous transverse figure of merit  $zT$  of  $\text{YbMnBi}_2$  compared to that of other high-ANE-performance compounds.

Third, present studies of good Heusler compounds in the thermoelectric society focus on the thermoelectric performance at high temperatures in a polycrystalline form, while their low temperature transport properties in a single crystal form, which can denote more intrinsic physical properties, have rarely been revealed. By growing high-quality Heusler single crystals, we can achieve a better understanding of their electronic structure and physical transport features.

Finally, further strategies, such as chemical doping to optimize the carrier concentration or tune the band structure, alloying to reduce the thermal conductivity and precisely control the magnetic structure or the strength of Berry curvature, applying a magnetic field, etc., can be reliable methods to enhance the thermoelectric performance as well as uncover unconventional transport properties.

## External Cooperation Partners

G. J. Snyder (Northwestern University, USA); Joseph P. Heremans (The Ohio State University, USA).

## References

- [1]\* *Mg<sub>3</sub>(Bi,Sb)<sub>2</sub> single crystals towards high thermoelectric performance*, Y. Pan, M. Yao, X. Hong, Y. Fan, F.-R. Fan, K. Imasato, Y. He, C. Hess, J. Fink, J. Yang, et al., *Energy Environ. Sci.* **13** (2020) 1717.
- [2]\* *Thermoelectric properties of novel semimetals: A case study of YbMnSb<sub>2</sub>*, Y. Pan, F.-R. Fan, X. Hong, B. He, C. Le, W. Schnelle, Y. He, K. Imasato, H. Borrmann, C. Hess, et al., *Adv. Mater.* **33** (2021) 2003168.
- [3] *Record anomalous Nernst signal in the antiferromagnet YbMnBi<sub>2</sub>*, Y. Pan, C. Le, B. He, S. J. Watzman, M. Yao, J. Gooth, J. P. Heremans, Y. Sun, and C. Felser, (2021) in progress.
- [4] *Spin-flop transition induced large anomalous Nernst effect in Dirac semimetal EuMnBi<sub>2</sub>*, D. Chen, B. He, Y. Pan, W. Schnelle, Y. Sun, and C. Felser, (2021) in progress.
- [5] *Giant anomalous Nernst effect in single crystal MnBi*, B. He, C. Şahin, S. R. Boona, B.C. Sales, Y. Pan, C. Felser, M.E. Flatté, and J. P. Heremans, *JOULE-D-21-00480*, under review, 2021.
- [6]\* *Revealing the intrinsic electronic structure of 3D half-Heusler thermoelectric materials by angle-resolved photoemission spectroscopy*, C. Fu, M. Yao, X. Chen, L. Z. Maulana, X. Li, J. Yang, K. Imasato, F. Zhu, G. Li, G. Auffermann, et al., *Adv. Sci.* **7** (2020) 1902409.
- [7] *Band structure of TiCoSb revealed by angle-resolved photoemission spectroscopy*, F. Serrano-Sanchez, M. Yao, Y. Pan, and C. Felser, (2021) in progress.

# Yu.Pan@cpfs.mpg.de